

# Electrostatic self-assembly of a ruthenium-based oxygen sensitive dye using polyion–dye interpolyelectrolyte formation

David A. Chang-Yen<sup>a,\*</sup>, Yuri Lvov<sup>b,1</sup>,  
Michael J. McShane<sup>c,2</sup>, Bruce K. Gale<sup>a,3</sup>

<sup>a</sup>Department of Mechanical Engineering, University of Utah, 50 S. Central Campus Drive, Room 2202, Salt Lake City, UT 84112-9208, USA

<sup>b</sup>Department of Chemistry, Institute for Micromanufacturing, Louisiana Tech University, 911 Hergot Avenue, Ruston, LA 71272, USA

<sup>c</sup>Department of Biomedical Engineering, Institute for Micromanufacturing, Louisiana Tech University, Ruston, LA 71272, USA

Received 22 April 2002; accepted 10 July 2002

## Abstract

The dye tris(2,2'-bipyridyl dichlororuthenium) hexahydrate has been successfully applied to glass and silica surfaces using the technique of layer by layer self-assembly. Solutions of both admixed polyion–dye and pure dye were used to attempt adsorption of the dye onto the substrates. Characterization of the constructed dye layers was performed using quartz crystal microbalance (QCM), UV-Vis absorbance spectrophotometry, fluorescence spectroscopy, and scanning electron microscopy (SEM) methods. Successive, controlled addition of multiple dye layers has been demonstrated, and exposure to different levels of dissolved oxygen shows that the films containing entrapped dye molecules retain sensing properties.

© 2002 Elsevier Science B.V. All rights reserved.

**Keywords:** Interpolyelectrolyte; Polyion; Ruthenium; Oxygen

## 1. Introduction

Detection of dissolved oxygen in a microscale environment is of considerable interest in the fields of microspectrophotometry and chromatography, enzyme activity monitoring, and cell culture [1–7]. Traditionally, dissolved oxygen sensing has been facilitated using Clarke-type amperometric oxygen sensors. This technology, though well established, is difficult to miniaturize, and has been carried out with only moderate success on the microscale [8–10]. Optical techniques show promise in overcoming the inherent shortcoming of the amperometric methodology, and organometallic compounds, particularly ruthenium-based dyes, have been demonstrated to exhibit fluorescence sensitivity to oxygen with very high chemical and pH selectivity [11–19].

However, the dimensions and patterning of immobilization films of fluorescent oxygen sensitive dyes to silicon-based substrates has proven difficult to control the microscale. Numerous methods of coating optical waveguides and platforms have been postulated, using techniques such as dipping, spinning and simple dropping to produce small areas of immobilized dye [11–19]. Of these techniques, only spinning is capable of producing a film of controllable, reliable thickness, but also suffers the disadvantage of producing relatively thick films, on the order of several microns. In the field of integrated sensors, as applied to microscale fluid flow, such irregularities are not acceptable, as small changes in a microfluid flow can greatly affect the overall operation of the device. Towards integrated optical oxygen sensing within cell culture substrates, layer-by-layer self-assembly permits spatially controlled deposition of functional dye layers at specific areas, such as exposed sections of integrated waveguides, determined by the surface charge difference of the waveguides to the surrounding substrate.

Electrostatic self-assembly has demonstrated the capability of producing nanoscale polyelectrolyte layers with

\* Corresponding author. Tel.: +1-801-581-6441; fax: +1-801-585-9826.

E-mail addresses: changyen@uofu.net (D.A. Chang-Yen), ylvov@coes.latech.edu (Y. Lvov), mcshane@coes.latech.edu (M.J. McShane), gale@eng.utah.edu (B.K. Gale).

<sup>1</sup> Tel.: +1-318-257-5100; fax: +1-318-257-5104.

<sup>2</sup> Tel.: +1-318-257-5112; fax: +1-318-257-5104.

<sup>3</sup> Tel.: +1-801-581-5944; fax: +1-801-585-5944.

embedded functional molecules [20–23]. This layer-by-layer process utilizes the inherent surface charge of molecules in solution to produce adsorption onto a substrate with an opposing surface charge when immersed in the same solution. To produce more than one adsorbed layer, adsorbed molecules must reverse the surface charge at the substrate–solution interface. Small molecules, such as typical fluorophores, simply neutralize the substrate surface, prohibiting further surface adsorption. To remedy this problem, long polymeric molecules with regular surface charges along their length are used. In the case of these polyions, not all of the charges are neutralized by the substrate surface charge, and the existing charge state is reversed, which facilitates further adsorption by polyions of opposite polarity.

For this work, ruthenium-based dyes were explored for use in an oxygen sensitive film. Electrostatic assembly for embedding ruthenium dye molecules between polyelectrolyte layers has been carried out by Cooper, Yoo, Rubner, Lvov, Ariga and Lee [5,24–27], permitted by the strong charge of the dye at low pH values. Looking towards biomedical applications, a number of requirements were not met by the method presented in that work. First, a more neutral pH of 7.6 was required for our layer environment in this experiment, as the polyions have isoelectric points at non-neutral pH values. Second, the dye used the work does not demonstrate a strong responsivity to changing oxygen concentrations as required for tissue culture monitoring, which display very small changes in dissolved oxygen concentration. Third, a dye with a stable surface charge and high water solubility was needed. The dye used for this experiment tris(2,2'-bipyridyl dichlororuthenium) hexahydrate, met all of these requirements, but has only a point positive charge of magnitude 2, as opposed to multiple charges present on the polyion molecules required to perform electrostatic layer-by-layer assembly. Accordingly, in this paper, we have shown that using a technique of admixing the dye with a strongly negative polyion to produce molecularly large interpolyelectrolyte complexes allows the dye to be adsorbed to silica surfaces in nanoscale increments while maintaining the dye's fluorescent characteristics. Oxygen sensitivity measurements of the dye have also been carried out to determine whether the layered state of the dye affects its sensitivity and overall response.

## 2. Methodology

The tris(2,2'-bipyridyl ruthenium) cation in solution, while bearing a strong positive surface charge at approximately neutral pH, is too small to cause surface charge inversion, and thus was mixed with a negatively charged polyion, poly(sodium styrenesulfonate), to form an *interpolyelectrolyte complex* that bears a net negative charge. A diagram of how the ruthenium dye and the PSS molecules may interact is shown in Fig. 1.

The interpolyelectrolyte complex is capable of adsorbing to an oppositely charged surface and causing surface charge inversion, as described in Ariga et al. [25]. Formation of interpolyelectrolyte complexes is based on spontaneous polymer complex formation in water, when charges of one component are in access to charges of another component [22]. The oxygen sensitive dye tris(2,2'-bipyridyl dichlororuthenium) hexahydrate (Ru(bpy)) was purchased from Aldrich in crystalline form and used in solution, both alone and mixed with the polyanion poly(sodium styrenesulfonate) (PSS; Sigma–Aldrich). The specifications for the polyions used were as follows: poly(ethylenimine) (PEI) of molecular weight 70,000 at 1.5 mg/ml, poly(sodium styrenesulfonate) (PSS) of molecular weight 500,000 at 3 mg/ml, and poly(diallyl dimethylammonium) chloride (PDDA) of molecular weight 70,000 at 2 mg/ml (Sigma–Aldrich). All the polyions used in the work were strongly charged at pH 6–8 [28]. The chemical structures for the materials used in this paper are given in Fig. 2.

All solutions were prepared at pH 7.6 (buffered with Trizma base and HCl buffer; Aldrich). The ruthenium layering solutions were prepared in four forms: in solution alone at 11.4 mg/ml and admixed with PSS at concentrations of 0.14, 0.28, and 0.57 mg/ml, corresponding to ratios of 80:1, 40:1, and 20:1 polyion monomeric units per molecule of ruthenium. Each of the polyion solutions were prepared from dry salts as received from Sigma–Aldrich with buffered water, excepting PEI, that was mixed from a 40 wt.% solution. The substrates chosen for the layering process were glass slides, each 2 in. × 3/8 in. cut from 1 in. × 3 in. × 1 mm Swiss glass (Fisher Scientific) microscope slides and cleaned in a solution of 60% H<sub>2</sub>O, 39% methanol, and 1% KOH for 20 min at 40 °C with sonication. The slides were then washed in flowing deionized water for 3 min, and dried under flowing N<sub>2</sub>.

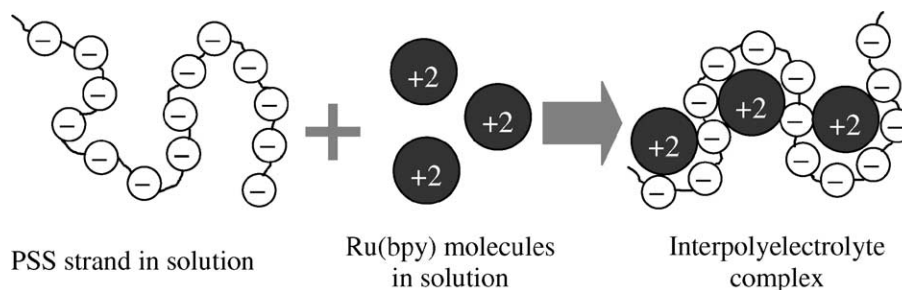


Fig. 1. Interpolyelectrolyte formation.

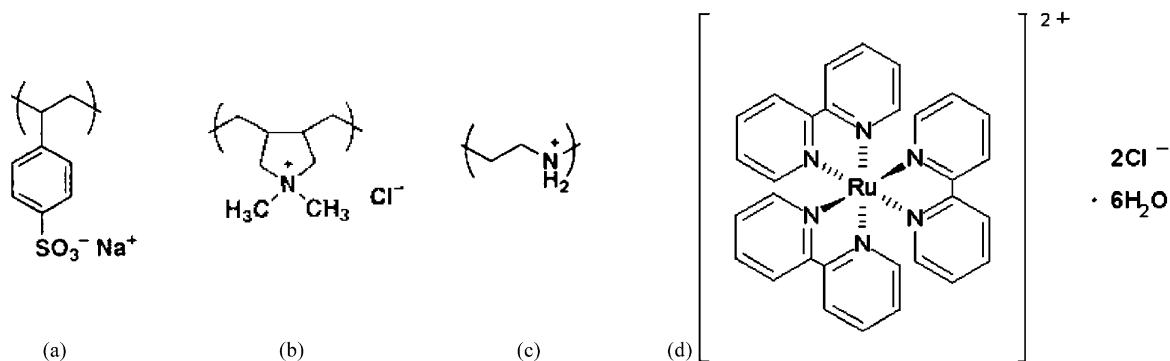


Fig. 2. Structural images of polyion and dye molecules (a) poly(sodium styrenesulfonate), (b) poly(diallyl dimethylammonium) chloride, (c) poly(ethylenimine), and (d) tris(2,2'-bipyridyl) dichlororuthenium hexahydrate.

Preparatory layers of PEI, PSS and PDDA were applied identically to all test slides to saturate the surfaces with a uniform charge. The slides were each immersed in the polyion solutions, allowing the charged polyions to adsorb to the oppositely charged surface. Irregular patches of surface charges on the substrate were inverted by the preparatory layers, and thus produced a uniform surface charge in preparation for the dye–polyion layering process. Microscopic inspection of the films following application of the dye layers verified uniform coverage of the glass substrates. The five preparatory layers (precursor) [29] shown in Table 1 were applied to each slide.

### 2.1. Admixed dye layering procedure

Three slides prepared according to Table 1 were layered with the three admixed PSS–Ru(bpy) solutions, respectively. The slides were dipped in the Ru(bpy)–PSS solutions and left for 20 min to ensure complete surface saturation and charge inversion. They were then removed and washed in pH 7.6-buffered deionized water twice for 30 s and dried with flowing nitrogen. This process produced thin PSS–Ru(bpy) monolayers on the slide surfaces with the slide surface charge inverted from positive to negative. The slides were then dipped into the PDDA solution for 20 min, then washed and dried similarly. These alternating layers thus served to invert the surface charge back to positive in preparation for a further PSS–Ru(bpy) dye layer adsorption. This process was

repeated 20 times to produce 20 functional dye layers on the slide, of 45 total monolayers, including the preparatory layers. Prior to dye–polyion layering, and after every five PSS–Ru(bpy)/PDDA bilayers were applied, the slide was scanned using a laser excitation apparatus (described later) for fluorescence emission changes. These scans were saved separately for later analysis.

### 2.2. Direct-assembly Ru(bpy) dye layering process

Another slide, designed to act as a control, was initially covered with similar preparatory layers as the admixed slides, and then layered with direct-assembly of the Ru(bpy) dye in solution using the concentrated Ru(bpy) solution and PSS polyion solution. To facilitate the first layer of Ru(bpy) on the slide, a layer of PSS was first applied to invert the surface charge from positively charged to negatively charged. The slide was dipped in the Ru(bpy) solution and left for 20 min to ensure complete surface saturation. It was then removed and washed in pH 7.6-buffered deionized water twice for 30 s and dried with flowing nitrogen. Following this first monolayer, the dye and PSS was applied five times in discrete bilayers, with fluorescence emission scans taken after application of every Ru(bpy)–PSS bilayer.

### 2.3. QCM tests

The two dipping methods described earlier were used for quartz crystal microbalance (QCM) dye-layering tests: direct-assembly and admixed dye layering. The admixed solution used was Ru(bpy)–PSS at 0.57 mg/l and PDDA which, when combined with the direct-assembly Ru(bpy) dye process, was used to evaluate the efficiency of the admixing process compared to direct-assembly. Two quartz crystals, AT-cut, resonant frequency 9 MHz, with silver electrodes were used as substrates for the QCM dye layering. The crystals were resonated using a USI-System Inc., Japan, 9 MHz RF generator, and monitored for resonance with an Iwatsu SC-7201 Universal Counter. Dye layering was restricted to the quartz crystal surfaces

Table 1  
Substrate and polyion surface charges for preparatory layers

Layer applied	Charge
Bare slide (no layers)	±
PEI	+
PSS	–
PDDA	+
PSS	–
PDDA	+

and contacts alone to prevent short-circuiting the electrode connections. QCM frequencies were measured in air after drying of the film. Once the five prep layers had been applied, measurements of crystal resonance were taken after each monolayer was applied, beginning with the prep layers alone and subsequently after each dye–polyion layer. Five dye–polyion bilayers were applied to each of the crystals. All the measurements were carried out in a climate-controlled room at 20 °C. The thickness and mass were determined from the QCM reading by using the Sauerbrey equation [30]:

$$\Delta F = \frac{-2F_0^2 \Delta M}{A\sqrt{\rho_q \mu_q}} \quad (1)$$

where  $\Delta F$  is the change in frequency from the original resonant frequency in Hz;  $F_0$  the quartz crystal's base resonant frequency, equal to 9 MHz;  $\Delta M$  the mass of the applied adlayer in nanograms;  $A$  the surface area of the crystal, calculated to be 0.16 cm<sup>2</sup>;  $\rho_q$  the density of quartz, equal to 2.65 g cm<sup>-3</sup>; and  $\mu_q$  is the shear modulus of quartz, equal to  $2.95 \times 10^{11}$  dyn cm<sup>-2</sup>. Using these values, simplified conversions for  $\Delta F$  to changes in layer thickness  $\Delta t$  and mass  $\Delta M$  were produced:

$$\Delta F(\text{Hz}) = -0.87 \Delta M(\text{ng}) \quad (2)$$

Direct scanning electron microscope scaling of polyion film thickness gives the following formula:

$$\Delta t(\text{nm}) = -0.016 \Delta F(\text{Hz}) \quad (3)$$

which is close to the theoretical one Eq. (2).

Observation of Eqs. (2) and (3) reveals that increases in mass to the surface of the crystal will cause decreases in the resonant frequency. Changes in the frequency observed during QCM testing were thus normalized and plotted.

#### 2.4. Optical absorption tests

Optical absorbance tests were carried out using an Agilent 8453 absorption spectrometer, using a 10 mm path length cell over a range of 200–1000 nm. The slides were placed perpendicular to the beam pathway, and the system was zeroed using a blank glass slide. To evaluate the effect of the self-assembled polyions layers and dye molecules separately on the optical absorption of the substrates, two slides were layered: the first with the five prep layers plus nine PSS and PDDA bilayers and the second with the prep layers and nine Ru(bpy)–PSS and PDDA bilayers, with the Ru(bpy) dye solution at 0.57 mg/ml concentration. To provide an optical absorbance reference for the three polyion-layered, a clean glass slide was used. The combination of these three slides allowed us to accurately determine changes in the absorbance of the dye components separately from the polyion layers and glass substrate. However, determination of effects on absorbance of the bilayers with increasing dye concentration was not evaluated, and is yet to be tested in the future.

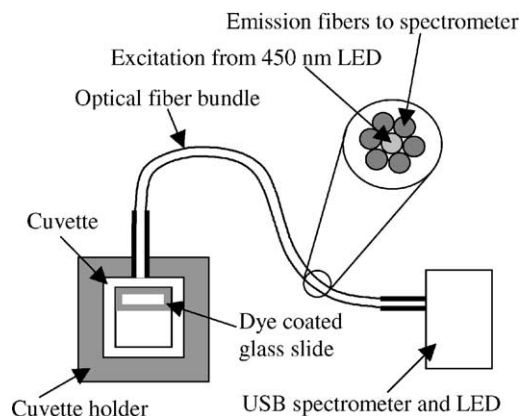


Fig. 3. Laser excitation and fluorescence scanning apparatus.

To assess possible changes of the immobilized fluorophore's quantum yield through self-quenching, a fifth slide was layered with 20 Ru(bpy)–PSS and PDDA bilayers, at a dye concentration of 0.57 mg/ml. Absorbance and fluorescence readings were taken after the application of every fifth layer and the absorbance intensity was plotted against increasing fluorescence intensity.

#### 2.5. Fluorescence tests

Following application of the preparatory polyion layers, the admixed and direct-layered slides were scanned for baseline fluorescence emission (zero dye layers), under excitation of 450 nm light. The optical system is setup as shown in Fig. 3. Excitation energy of the dye at 450 nm was produced with an Ocean Optics LS-450-USB LED light source. The excitation pulse was directed normally to the slide surface through the center fiber of the optical fiber bundle, and the resulting fluorescence emission light was collected by the surrounding six fibers. This arrangement allowed very stable, repeatable fluorescence measurements to be taken for multiple slides. All fluorescence measurements were scanned with an Ocean Optics USB2000 Fiber Optic Spectrometer over a 340–1000 nm wavelength range using a 1000 ms integration period and a 10-point average.

#### 2.6. Scanning electron microscopy (SEM) imaging

To provide a visual measurement of the thickness of the layers, an scanning electron microscopy (SEM; AMRAY) image was taken of the 0.28 mg/ml dye–polyion-layered absorbance glass slide that had been cleaved through the polyion layers. These images were taken to provide final thickness measurements of the 20 completed polyion bilayers, plus the prep layers. The SEM image also allowed us to visually gauge the effects of the incorporated dyes into the polyion layers, supported by the QCM readings.

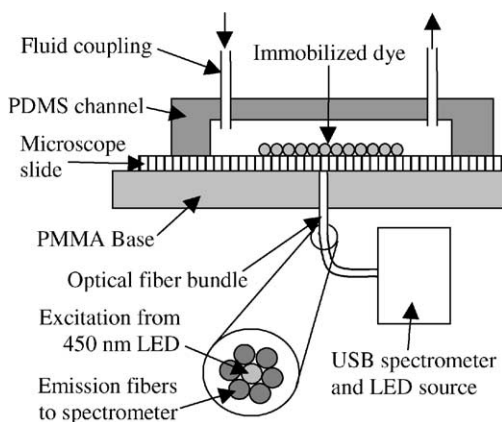


Fig. 4. Controlled dissolved oxygen testing apparatus.

### 2.7. Oxygen sensitivity tests

Using the 0.57 mg/ml concentration ruthenium dye–polyion solution, a full size (1 in.  $\times$  4 in.) Swiss glass (Fisher Scientific) microscope slide was layered at the center of one of the slide surfaces. Strips of adhesive tape were used to restrict the dye layering to a small area at the center of the slide surface, corresponding to a section of the wall of the completed controlled oxygen fluid testing apparatus (Fig. 4). The same dye layering methodology was used for this substrate as was used for the smaller fluorescence and absorption test substrates.

A water/gas-mixing closed-loop system was used to provide a controlled dissolved oxygen liquid environment. Oxygen and nitrogen were bubbled into and dissolved in deionized water in a stirred chamber that was monitored with a dissolved oxygen probe (VWR Scientific Instruments). The actual oxygen concentration was monitored using the probe, and the gas flow rates were adjusted to provide the desired dissolved oxygen concentrations. The fluid was then pumped out the chamber and into the testing apparatus shown in Fig. 4. Fluid out of the apparatus was sent back to the mixing chamber, creating a closed fluid loop.

The PDMS channel of the controlled oxygen loop was fabricated using a peel-off acrylic plastic mold, and sealed to the glass slide using a pressure clamp. The fluid couplings were attached to the channel using a cyanoacrylate-based epoxy. No fluid leakage was observed during testing, even using flow rates as high as 7.3 ml/min, that was required to reduce the effect of oxygen diffusion through the edges of the PDMS channel. Care was taken during integration of the optical fiber to the PMMA base to minimize the gap between the tip of the fiber and the underside of the glass substrate by screwing in the optical fiber bundle until the fiber end faces were pressed firmly against the microscope slide. The known oxygen concentration that was pumped into the test apparatus ranged from 0.6 to 10.8 mg/l with steps of approximately 1 mg/l, which allowed us to determine the oxygen sensitivity of the dye-layered substrate for a dissolved oxygen range of approximately 0–25%.

## 3. Results and discussion

### 3.1. QCM

The first tests carried out to completion were the QCM tests, which provided firm indications to the success of the dye layering. A clear upward trend of the Ru(bpy)–PSS at 0.57 mg/ml concentration and PDPA dye solutions show that surface adsorption to the slide was occurring (Fig. 5), with no evidence of dye desorption. Comparison of this plot to previously accomplished work by Ariga et al. [27] of layer-by-layer self-assembly of PSS and PDPA show similar trends, indicating that the addition of the ruthenium dye to the PSS polyion layers does not adversely affect the layering process.

However, in the case of the concentrated ruthenium solution (direct-assembled dye), this trend was not present, indicative of failed layer adsorption. Considering the nature of the alternately charged layer-by-layer adsorption process, this adsorption failure is not unpredictable. According to Ariga et al. [25], for successive layers to be applied to a charged surface, the applied layer must not only adsorb to the surface, but also invert the surface charge. The ruthenium molecule is relatively small dication as compared to any of the polyions. Hence, instead of surface charge inversion, surface charge neutralization takes place, preventing any further layer adsorption [31].

The y-axis of the data plot in Fig. 5 is normalized to display an upward trend in the layer thickness. Calculation of the average layer thickness using Eq. (3) yielded surprisingly low values (Table 2), compared to the calculated result of 22 nm (for all layers adsorbed to the slide) from the SEM imaging. This discrepancy is most likely caused by the assumption that the adsorbed layer density is similar to the quartz resonator density. The interpolyelectrolyte layering process will yield characteristically much lower density

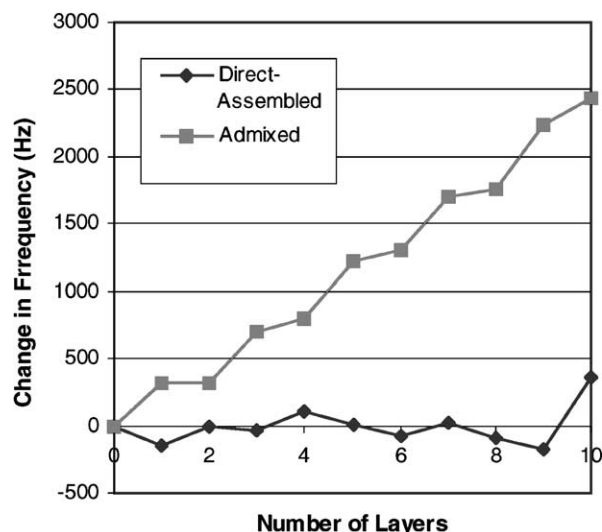


Fig. 5. QCM plots of direct-assembled and admixed dye.

Table 2  
QCM summary

Layer applied	Normalized average thickness (nm)
Admixed PDDA	1.4848
Admixed dye–PSS	6.3264
Direct-assembled dye	0.0845
Direct-assembled PSS	0.8256

layers, as the packing of the polyions onto the surface will be much looser, around the complexes. Additionally, the initial polyion layer applied to the slide, PEI, has a highly branched structure that could also decrease the total average layer density.

### 3.2. Optical absorption

The optical absorption data provided the first indication of successful adsorption (Fig. 6). As expected, the clean reference slide shows no significant absorption. Low-level absorption is produced by the PSS and PDDA layered slide. In contrast, the Ru(bpy)–PSS and PDDA layered slide shows strong adsorption at the excitation wavelength of 460 nm. The strong optical absorption measurements demonstrate not only that the layers are assembled as expected, but also indicate that the assembly process does not adversely impact the fluorescent functions of the ruthenium dye.

The results from the self-quenching absorbance–fluorescence tests are shown in Fig. 7. Absorbance of the coated slide (not shown) increased in a linear fashion with increasing number of dye layers, and this trend was maintained with increasing fluorescence intensity. The constant relationship between the dye's absorbance and fluorescence, indicative of unchanging quantum yield, conclusively illustrates that despite the high concentration of dye molecules in the assembled bilayers self-quenching of the dye at a concen-

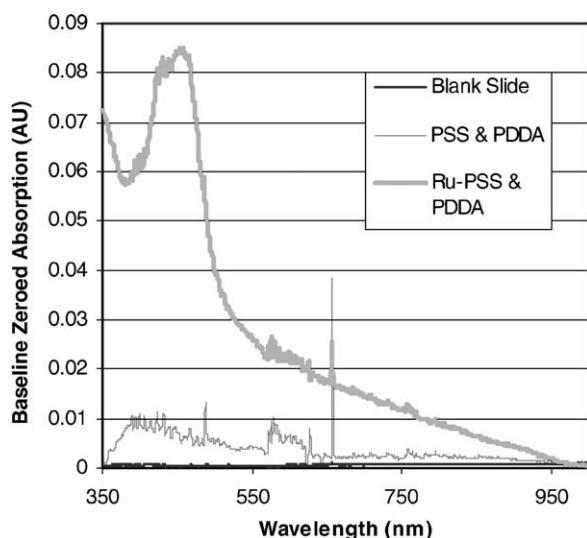


Fig. 6. Absorbance spectra of polyion-coated glass substrates.

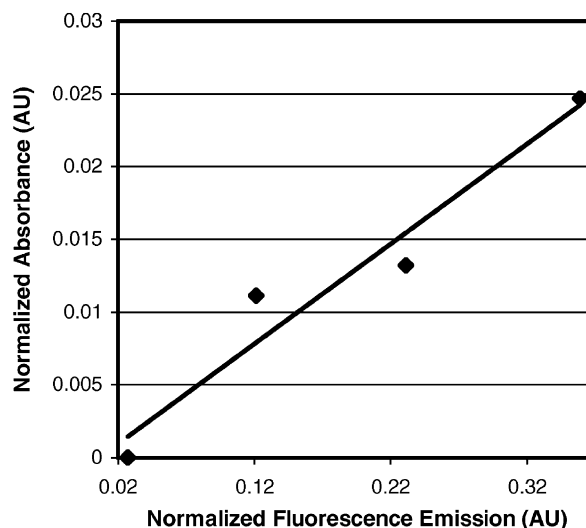


Fig. 7. Plot of normalized dye absorbance against normalized fluorescence emission for increasing dye layers.

tration of 0.57 mg/ml was not observed. This result demonstrates that operation of an oxygen sensor within the tested range of dye concentration is feasible, but determination of the self-quenching limit of the dye in the bilayers requires further testing is required with increased Ru(bpy) concentrations.

### 3.3. Direct-assembly Ru(bpy) dye layering fluorescence

As exhibited in Fig. 8, despite repeated applications of polyion–dye bilayers, no change occurred in the spectra at 610 nm, the wavelength at which the ruthenium dye fluorescence shows peak emission. Additionally, the remaining PSS dipping solution from this direct-assembled slide shows a large fluorescent emission peak at 610 nm, demonstrating that the ruthenium dye was desorbing from the surface into the PSS dipping solution.

### 3.4. Admixed dye–polyion layer fluorescence

Despite increased neutralization of the PSS polyions by the Ru(bpy) dye molecules, surface adhesion and subsequent layer formation is uninhibited. Furthermore, as shown in Fig. 9, a uniform increase in intensity was observed for the 1:20 concentration dye–polyion mixture. In support, comparative study of the effects of varying Ru(bpy)–PSS ratios on fluorescence emission intensity (Fig. 10) demonstrates expected trends in fluorescence with increasing dye concentration.

Supported by the QCM data, all admixed dye layers show definitive increases with increasing numbers of layers, while the direct-assembly process fails to produce any substantial fluorescent response. Since the emission intensity continues to climb as the ratio of ruthenium molecules to polyion mer units falls, there may be an even lower ratio that would

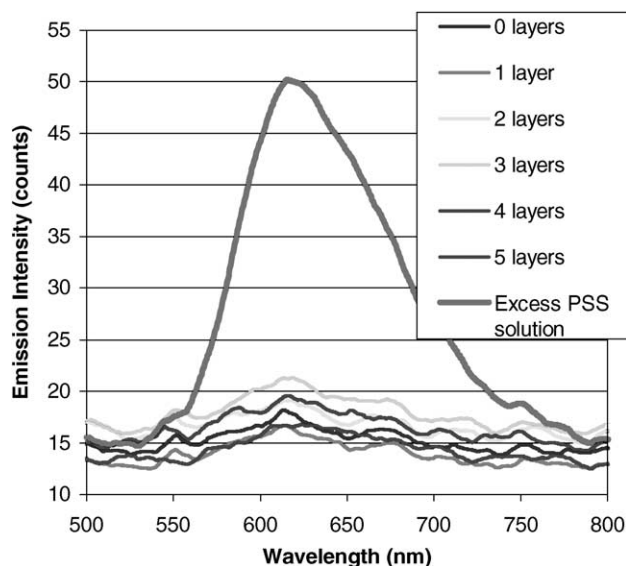


Fig. 8. Direct-assembly dye fluorescence spectra.

provide the maximum level of emission intensity and corresponding dye concentration. We are currently exploring these lower ratio combinations to see if the emission intensity might be further enhanced, while remaining below the self-quenching concentration limit.

### 3.5. SEM imaging

Using the SEM images in Fig. 11b, the final thickness of the dye–polyion layers is estimated to be 1  $\mu\text{m}$ , corresponding to an average monolayer thickness of 22 nm. The SEM image also reveals very uniform surface coverage by the

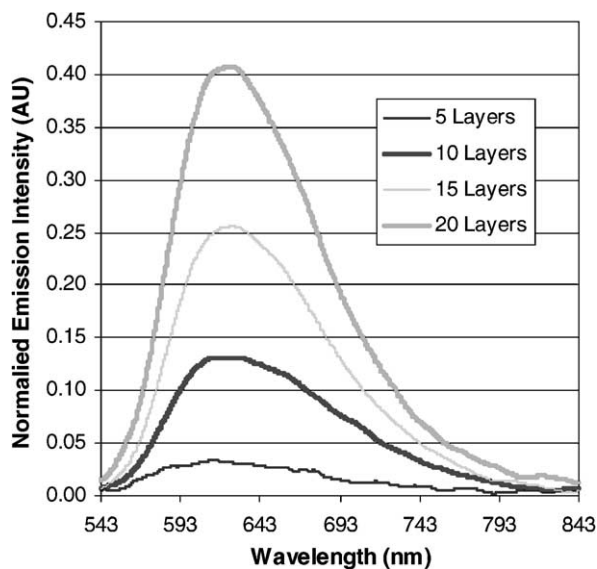


Fig. 9. The 1:20 admixed dye–polyion fluorescence intensity trend with increasing number of adsorbed layers.

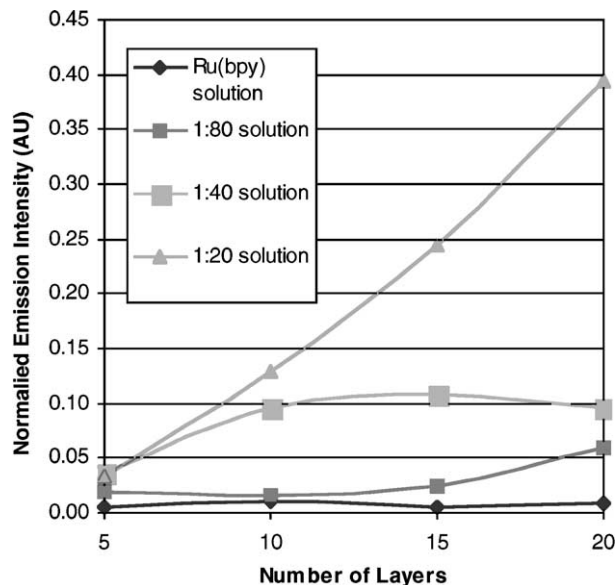
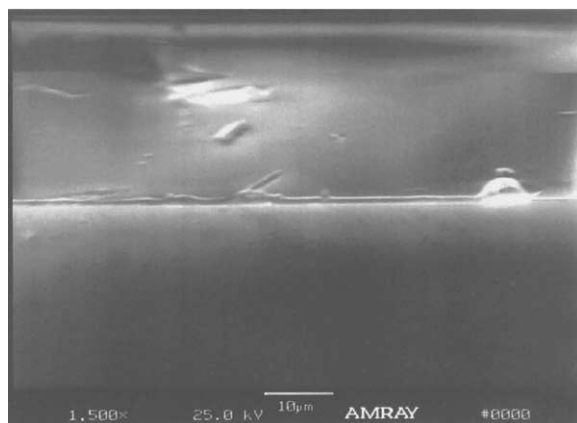


Fig. 10. Comparative fluorescence plots of varying admixed polyion concentrations.

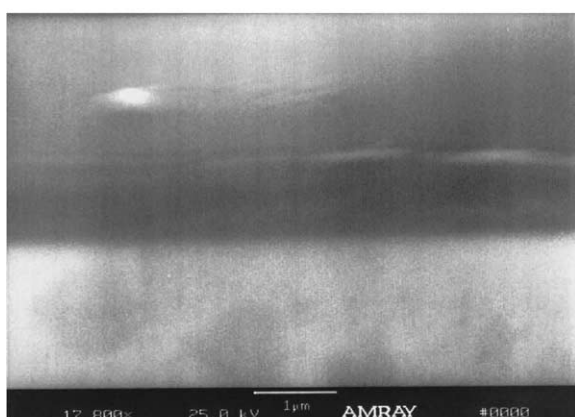
dye–polyion layers, even over trapped dust particles (center, Fig. 11a). Despite the apparent thinness of these layers, the dye is densely concentrated in the polyion layers, and is readily visible on the glass substrate without magnification using transmitted light. As explained earlier, this total average layer thickness of 22 nm did not directly correlate with the QCM results, but can be possibly explained by the increased true density by the interpolyelectrolyte complex and PEI preparatory layer.

### 3.6. Oxygen sensitivity

Oxygen sensitivity of the immobilized dye was observed over the tested range, and a calibration plot for the test apparatus was thus obtained (Fig. 12). Within the dissolved oxygen range chosen, the plotted values show a standard error of only 15.036 counts. According to previously published work [15,16], calibration plots have only been produced for minimum changes in oxygen concentration of 10%; in comparison, the calibration plot corresponds to changes of less than 3%. Considering that changes in oxygen concentration in cell cultures are typically less than 10%, this increased resolution offers a much more accurate method of testing dissolved oxygen concentrations within biological environments. Additionally, linear regression of the data displays a Stern–Volmer-type trend, demonstrated by the strong linearity of the plot. Currently, mathematical modeling of the Stern–Volmer relationship against the data plot is being carried out, to determine if the oxygen sensitivity characteristics are affected by the immobility of the dye. In terms of stability of the films, the oxygen sensitivity testing was carried out over a period of several hours per full range test, with fully repeatable sensitivity being displayed by the film, despite the high fluid shear applied on the film by



(a)



(b)

Fig. 11. SEM images of the cleaved glass substrates, showing the dye-polyion layers: (a) 1500 $\times$  magnification, and (b) 17,000 $\times$  magnification.

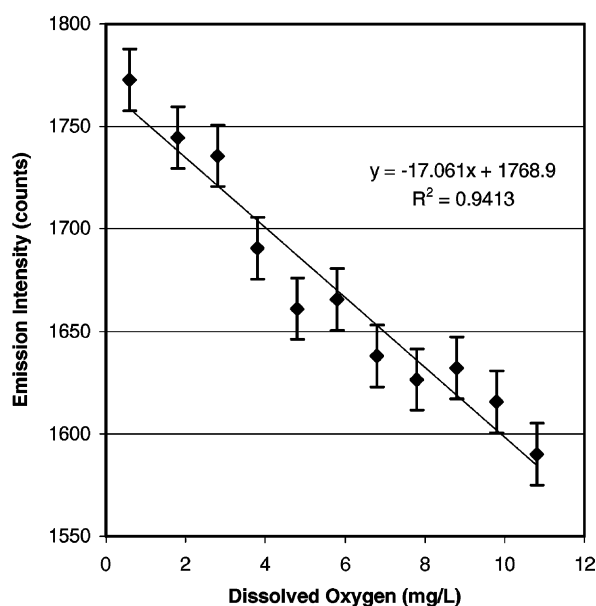


Fig. 12. Calibration plot of fluorescence emission intensity vs. dissolved oxygen concentration showing standard error of emission intensity.

the water. Additionally, due to the extended time required to carry out the oxygen sensitivity testing, on the order of 5–6 h, several days were required to complete all sensitivity tests. Over that period, no noticeable degradation in oxygen responsivity was observed, and the films showed similar fluorescent emission spectra even after repeated disassembly and reassembly of the flow cell. Testing for photobleaching and chemical and pH stability is planned in future work, and possibly interference of foreign media, such as organics and corrosive materials.

#### 4. Conclusions

Using the process of layer-by-layer self-assembly, the oxygen-sensitive dye tris(2,2'-bipyridyl dichlororuthenium) hexahydrate, complexed with various polyions was successfully adsorbed onto glass substrates, in the form of ultrathin dye-polyion layers. The layering process was shown to be highly controllable, with average dye-polyion layer thickness increases of 22 nm per layer, according to SEM measurements. The completed dye-polyion layers displayed characteristic low surface roughness and very good surface coverage of the test substrates. Oxygen sensitivity of the immobilized dye was maintained, and a calibration plot was produced. The direct-assembly of the oxygen-sensitive dye with poly(sodium styrenesulfonate) was not successful, highlighting the usefulness of the admixing process. Under the conditions used, efficient ruthenium dye assembly was not observed for indirect interactions between ruthenium and adsorbed polyanions. In contrast, pre-mixing of the ruthenium dye with the polyanion PSS allowed the formation of *interpolyelectrolyte complexes*, which were then successfully deposited in alternation with the polycation PDDA to achieve functional fluorescent layers.

The method demonstrated here for immobilizing the ruthenium dye could potentially be used for a large number of other dyes with sensitivity to other species. Accordingly, 1 nm thick layers could potentially contain dyes sensitive to an array of analytes, and accordingly, techniques in lithographic patterning are currently being investigated to assess the capabilities of this oxygen sensing system to integrated arrays. Such sensing arrays could be invaluable in developing multi-analyte, high-resolution sensors with applications in medicine, biology, chemistry, and engineering.

#### Acknowledgements

This material is based upon work supported in part by National Science Foundation Grant no. 0092001 "Micro/Nanodevices and Systems". Any opinions, findings, and conclusions or recommendations expressed in this material are those of the authors and do not necessarily reflect the view of the National Science Foundation.

## References

- [1] M. Thieme, Transformations of titanium carbide precipitations under hydrothermal conditions, *Corros. Sci.* 34 (1993) 383–389.
- [2] I. Karube, Development of new microbiosensors, *Polym. J.* 23 (1991) 573–581.
- [3] A. Neubauer, D. Pum, U.B. Sleytr, I. Klimant, O.S. Wolfbeis, Fibre-optic glucose biosensor using enzyme membranes with 2D crystalline structure, *Biosens. Bioelectron.* 11 (1996) 317–325.
- [4] M. Sudoh, A. Mori, H. Fujimura, H. Katayama, Development of novel micro-sensor of disposable chips with oxygen enrichment by pre-electrolysis for monitoring blood glucose, *Electrochim. Acta* 44 (1999) 3839–3848.
- [5] H. Sukuki, H. Arakawa, I. Karube, Fabrication of a sensing module using micromachined biosensors, *Biosens. Bioelectron.* 16 (2001) 725–733.
- [6] X. Gu, Y. Chen, Interactive control of pH and DO in the animal cell culture, *J. East China Inst. Chem. Tech.* 15 (1989) 498–503.
- [7] B.A.A. Dremel, S.-Y. Li, R.D. Schmid, On-line determination of glucose and lactate concentrations in animal cell culture based on fibre optic detection of oxygen in flow-injection analysis, *Biosens. Bioelectron.* 7 (1992) 133–139.
- [8] T. Hermes, M. Buhner, S. Bucher, C. Sundermeier, C. Dumschat, M. Borchardt, K. Cammann, M. Knoll, An amperometric microsensor array with 1024 individually addressable elements for two-dimensional concentration mapping, *Sens. Actuators B: Chem.* 21 (1994) 33–37.
- [9] H. Suzuki, T. Hirakawa, T. Hoshi, H. Toyooka, Micro-machined sensing module for  $pO_2$ ,  $pCO_2$ , and pH and its design optimization for practical use, *Sens. Actuators B: Chem.* 76 (2001) 565–572.
- [10] P.R. Warburton, R.S. Sawtell, A. Watson, A.Q. Wang, Failure prediction for a galvanic oxygen sensor, *Sens. Actuators B: Chem.* 72 (2001) 197–203.
- [11] I. Klimant, G. Holst, M. Kuhl, Oxygen microoptodes and their application in aquatic environment, *Soc. Photo-Opt. Instrum.* 2508 (1995) 375–386.
- [12] G. Holst, M. Kuhl, I. Klimant, A novel measuring system for oxygen microoptodes based on a phase modulation technique, *Soc. Photo-Opt. Instrum.* 2508 (1995) 387–398.
- [13] M.T. Murtaugh, H.C. Kwon, M.R. Shahriari, Luminescence probing of organically-modified sol-gel thin films for sensing applications, *Soc. Photo-Opt. Instrum.* 3136 (1997) 187–198.
- [14] B. Hannemann, A. Tamachkiarowa, C. Radelhaus, Comparison between stationary intensity and lifetime luminescence measurements with fiber optic oxygen sensors, containing  $[Ru(4.7 Ph_2 phen)_3]^{2+}$  in silicone polymer, *Soc. Photo-Opt. Instrum.* 2508 (1995) 291–302.
- [15] A.K. Asundi, J.W. Chen, D.M. He, Fibre optic spectrophotometry monitoring dissolved oxygen in tropical ornamental fish tank environment, *Soc. Photo-Opt. Instrum.* 3740 (1999) 561–564.
- [16] A.K. McEvoy, C.M. McDonagh, B.D. MacCraith, Development of a fibre-optic oxygen sensor based on quenching of a ruthenium complex entrapped in a porous sol-gel film, *Soc. Photo-Opt. Instrum.* 2508 (1995) 190–198.
- [17] S. Dourado, R. Kopelman, Development of fluorescent fiber-optic single polymer membrane sensors for simultaneous ratiometric detection of oxygen and carbon dioxide in biological systems, *Soc. Photo-Opt. Instrum.* 3540 (1999) 224–234.
- [18] Z. Murtaza, J.R. Lakowicz, Lifetime-based sensing of glucose using luminescent ruthenium(II) metal complex, *Soc. Photo-Opt. Instrum.* 3602 (1999) 326–334.
- [19] P.A. Wallace, Y. Yang, M. Campbell, Towards a distributed optical fibre chemical sensor, *Soc. Photo-Opt. Instrum.* 2508 (1995) 36–40.
- [20] T.M. Cooper, A.L. Campbell, R.L. Crane, Formation of polypeptide-dye multilayers by an electrostatic self-assembly technique, *Langmuir* 11 (1995) 2713–2718.
- [21] E.S. Handy, A.J. Pal, M.F. Rubner, Solid state light-emitting devices based on the tris-chelated ruthenium(II) complex. 2. Tris(bipyridyl) ruthenium(II) as a high-brightness emitter, *J. Am. Chem. Soc.* 121 (1999) 3225–3227.
- [22] V. Kabanov, *Macromolecular Complexes in Chemistry and Biology*, in: P. Dubin, J. Block, R. Davies, D. Schulz (Eds.), Springer, Berlin, 1994, pp. 151–174.
- [23] G. Decher, Fuzzy nanoassemblies: toward layered polymeric multicomposites, *Science* 227 (1997) 1232–1237.
- [24] D. Yoo, J.L. Lee, M.F. Rubner, Investigations of new self assembled multiplayer thin films based on alternately adsorbed layers of poly electrolytes and functional dye molecules, *MRS Symp. Proc.* 413 (1996) 395–400.
- [25] K. Ariga, Y. Lvov, T. Kunitake, Assembling alternate dye-polyion molecular films by electrostatic layer-by-layer adsorption, *J. Am. Chem. Soc.* 119 (1997) 2224–2231.
- [26] S.-Y. Lee, J. Kumar, S.K. Tripathy, Thin film optical sensors employing polyelectrolyte assembly, *Langmuir* 16 (2000) 10482–10489.
- [27] K. Ariga, M. Onda, Y. Lvov, T. Kunitake, Alternate layer-by-layer assembly of organic dye and proteins is facilitated by premixing with polyions, *Chem. Lett.* (1997) 25–26.
- [28] Y. Lvov, K. Ariga, I. Ichinose, T. Kunitake, Assembly of multi-component protein films by means of electrostatic layer-by-layer adsorption, *J. Am. Chem. Soc.* 117 (1995) 6117–6122.
- [29] Y. Lvov, G. Decher, H. Möhwald, Assembly, structural characterization and thermal behavior of layer-by-layer deposited ultrathin films of polyvinylsulfonate and polyallylamine, *Langmuir* 9 (1993) 481–486.
- [30] Y. Okahata, H. Ebato, Detection of bioactive compounds using a lipid-coated quartz-crystal microbalance, *Trends Anal. Chem.* 11 (1992) 344–355.
- [31] M. Linford, M. Auch, H. Möhwald, Nonmonotonic effect of ionic strength on surface dye extraction during dye-polyelectrolyte multilayer formation, *J. Am. Chem. Soc.* 120 (1998) 178–182.

## Biographies



David A. Chang-Yen received his BS and MS degrees in biomedical engineering from Louisiana Tech University, Ruston in 2000 and 2002, respectively, and is currently working towards completion of his PhD in mechanical engineering from the University of Utah, Salt Lake City. David's research focus includes BioMEMS, microfabricated optical biosensors, and microfabricated tissue culture platforms.



Yuri Lvov is associate professor in the Institute for Micromanufacturing, Louisiana Tech University. Earlier he worked in Naval Research Laboratory, Washington DC, in Japan Science Agency (JRDC), and in Mainz University, Germany. He is author and co-author of more than 100 scientific publications on ultrathin organized films, polymer nanocomposites and protein/polyion multilayers. Y. Lvov was among pioneers of the technique based on the layer-by-layer assembly by alternate adsorption of oppositely charged components.



*Michael J. McShane* is an assistant professor of biomedical engineering and a research associate at the Institute for Micromanufacturing, Louisiana Tech University. He has authored or co-authored over 40 scientific publications on spectroscopy, micro/nanofabrication, and signal processing as applied to biochemical measurements. His main research interests are analytical micro/nanodevices for detection, monitoring, and management of diseases, especially diabetes and brain disorders.



*Bruce K. Gale* received his BS in mechanical engineering from Brigham Young University in 1995 and a PhD in bioengineering from the University of Utah in 1999. He spent over 2 years as an assistant professor of biomedical engineering at Louisiana Tech University and the Institute for Micromanufacturing. In December 2001, he joined the Mechanical Engineering Department at the University of Utah. His interests include medical and biological-based applications of micromachining and his work has recently involved micromachined particle separation systems and detectors, MEMS for tissue engineering applications, and sensors related to these applications.